

Elastic pp and $\bar{p}p$ scattering in models with a unitarized Pomeron

E. Martynov*

Bogolyubov Institute for Theoretical Physics, 03680 Kiev, Ukraine

(Received 5 July 2007; published 22 October 2007)

Elastic scattering amplitudes dominated by the Pomeron singularity which obey the principal unitarity bounds at high energies are constructed and analyzed. Confronting the models of double and triple (at $t = 0$) Pomeron pole (supplemented by some terms responsible for the low energy behavior) with existing experimental data on pp and $\bar{p}p$ total and differential cross sections at $\sqrt{s} \geq 5$ GeV and $|t| \leq 6$ GeV² we are able to tune the form of the Pomeron singularity. Actually the good agreement with the data is received for both models though the behavior given by the dipole model is more preferable in some aspects. The predictions made for the LHC energy values display, however, the quite noticeable difference between the predictions of models at $t \approx -0.4$ GeV². Apparently the future results of TOTEM experiment will be more conclusive to make a true choice.

DOI: [10.1103/PhysRevD.76.074030](https://doi.org/10.1103/PhysRevD.76.074030)

PACS numbers: 13.85.Dz, 11.55.Jy, 13.60.Hb, 13.85.-t

I. INTRODUCTION

The forthcoming TOTEM experiment at LHC will provide us with the first measurements of soft Pomeron (strictly speaking Pomeron and odderon) as the contributions of secondary reggeons are negligible at such high energies. Then obviously the precise measurement of pp differential cross section makes it possible to discriminate the various Pomeron models comparing their particular predictions. Certainly, such an analysis makes sense only if the same data set is used with the model parameters reliably fixed. For the time being there are three model types for elastic hadron scattering amplitudes which reproduce rising cross sections experimentally measured with a high precision.

- (i) Models treating Pomeron (and odderon as well) as a simple pole in a complex momentum plane located to the right of unity, $\alpha_p(0) = 1 + \varepsilon \approx 1.1$ [1,2]. In order to describe a dip-bump structure in differential cross section one should take into account the cuts in one or another form. Such a Pomeron violates unitarity bound $\sigma_t(s) \leq C \ln^2 s$ at $s \rightarrow \infty$. However, the argument that unitarity corrections are important only at higher energies justifies this approach.
- (ii) Pomeron with $\alpha_p(0) > 1$ is an input in some scheme of unitarization (for example, eikonal or quasieikonal [3], U -matrix models [4]). Having done the unitarization all such models give $\sigma_t(s) \propto \ln^2 s$, whereas other characteristic predictions depend on the concrete model.
- (iii) Another way to construct amplitude is just to take into account unitarity and analytical requirements from the beginning as well as experimental information on the cross sections (e.g., growth of total cross sections). We named such a model in what follows as the model of unitarized Pomeron. Here the most

successful examples are tripole Pomeron [$\sigma_t(s) \propto \ln^2 s$] [5–7] and dipole Pomeron [$\sigma_t(s) \propto \ln s$] [8,9].

Within the third approach we consider the models of tripole and dipole Pomeron. These models are most successful in a description of all data on the forward scattering data [10].

As has been shown [10,11] the total cross sections of meson and nucleon interactions are described with the minimal χ^2 in the dipole and tripole models in which forward scattering amplitudes are parametrized in explicit analytic form. This conclusion was confirmed by analysis applying the dispersion relations for the real part of amplitudes [12].

The elastic scattering at small $|t|$ ($0.1 \leq |t| \leq 0.5$ GeV²) (pp , $\bar{p}p$, $\pi^\pm p$, and $K^\pm p$) was analyzed in detail [13]. The particular model was considered as a combination of hard [with $\alpha_h(0) \approx 1.4$] and soft $\alpha_s(0) \approx 1.1$ Pomeron contributions. It was noticed in [14] that additional hard Pomeron essentially improves the description of the meson and nucleon data on parameter $\rho = \text{Re}A(s, 0)/\text{Im}A(s, 0)$ comparing with the ordinary soft Pomeron model. Extension of the model to higher $|t|$ can be done within some scheme of unitarization (e.g., eikonal, quasieikonal, U matrix) taking into account Pomeron rescatterings or cuts.

Here we focus on the dipole and tripole Pomeron models. Without presenting the details we note here these models describe the small- $|t|$ differential cross sections with the same level of precision [$\chi^2/\text{dof} \lesssim 1.05$; degrees of freedom (dof)] as the model of [13] did. The purpose of this paper is to demonstrate the description of the data on elastic pp and $\bar{p}p$ scattering at low and middle t in the dipole and tripole Pomeron models.

In Sec. II we present the general restrictions on hardness of Pomeron singularity and form of its trajectory at small t , imposed by unitarity bounds on cross sections. In Secs. III and IV parametrizations of pp and $\bar{p}p$ elastic scattering amplitudes are presented dealing with dipole and tripole

*martynov@bitp.kiev.ua

Pomeron models, correspondingly. Results of least square analysis for both models as well as their comparison are given in the Sec. V.

II. GENERAL CONSTRAINTS

Let us reiterate here that the model with $\sigma_t(s) \propto \ln^2 s$ is not compatible with a linear Pomeron trajectory having the intercept 1. Indeed, let us assume that

$$\alpha_p(t) = 1 + \alpha'_p t$$

and the partial wave amplitude develops the form

$$\begin{aligned} \varphi(j, t) &= \eta(j) \frac{\beta(j, t)}{[j - 1 - \alpha'_p t]^n} \approx \frac{i\beta(1, t)}{[j - 1 - \alpha'_p t]^n}, \\ \eta(j) &= \frac{1 + e^{-i\pi j}}{-\sin \pi j}. \end{aligned} \quad (1)$$

In (s, t) -representation amplitude $\varphi(j, t)$ is transformed to

$$a(s, t) = \frac{1}{2\pi i} \int dj \varphi(j, t) e^{\xi(j-1)}, \quad \xi = \ln(s/s_0). \quad (2)$$

Then, we have Pomeron contribution at large s as

$$a(s, t) \approx -g(t) [\ln(-is/s_0)]^{n-1} (-is/s_0)^{\alpha_p t}, \quad (3)$$

where

$$g(t) = \beta(t) / \sin(\pi \alpha_p(t)/2).$$

If as usual $g(t) = g \exp(bt)$ then we obtain

$$\sigma_t(s) \propto \ln^{n-1} s, \quad \sigma_{el}(s) \propto \frac{1}{s^2} \int_{-\infty}^0 dt |a(s, t)|^2 \propto \ln^{2n-3} s. \quad (4)$$

According to the obvious inequality,

$$\sigma_{el}(s) \leq \sigma_t(s), \quad (5)$$

we have

$$2n - 3 \leq n - 1 \Rightarrow n \leq 2. \quad (6)$$

Thus we come to the conclusion that a model with $\sigma_t(s) \propto \ln^2 s$ is incompatible with a linear Pomeron trajectory. In other words, the partial amplitude Eq. (1) with $n = 3$ (but used in some papers) in principle is incorrect.

If $n = 1$ we have a simple j pole leading to constant total cross section and vanishing elastic cross section. However, such a behavior of the cross sections is not supported by experimental data.

If $n = 2$ we have the model of dipole Pomeron [$\sigma_t(s) \propto \ln(s)$] and would like to emphasize that double j pole is the maximal singularity of partial amplitude settled by unitarity bound (5) if its trajectory is linear at $t \approx 0$.

Thus, constructing the model leading to cross section which increases faster than $\ln(s)$, we need to consider a more complicated case:

$$\begin{aligned} \varphi(j, t) &= \eta(j) \frac{\beta(j, t)}{[j - 1 + k(-t)^{1/\mu}]^n} \\ &\approx \frac{i\beta(1, t)}{[j - 1 + k(-t)^{1/\mu}]^n}. \end{aligned} \quad (7)$$

Making use of the same arguments as above, we obtain

$$\begin{aligned} \sigma_t(s) &\propto \ln^{n-1} s, \\ \sigma_{el}(s) &\propto \ln^{2n-2-\mu} s \quad \text{and} \quad \mu \geq n - 1. \end{aligned} \quad (8)$$

However in this case amplitude $a(s, t)$ has a branch point at $t = 0$ which is forbidden by analyticity.

A proper form of amplitude leading to t_{eff}^1 decreasing faster than $1/\ln s$ (it is necessary for σ_t to rise faster than $\ln s$) is the following

$$\varphi(j, t) = \eta(j) \frac{\beta(j, t)}{[(j-1)^m - kt]^n}. \quad (9)$$

Now we have m branch points colliding at $t = 0$ in j plane and creating the pole of order mn at $j = 1$ (but there is no branch point in t at $t = 0$). At the same time $t_{\text{eff}} \propto 1/\ln^m s$ and from the $\sigma_{el} \propto \ln^{2mn-2-m} s \leq \sigma_t \propto \ln^{mn-1} s \leq \ln^2 s$ one can obtain

$$mn \leq m + 1, \quad mn \leq 3. \quad (10)$$

If $\sigma_{el} \propto \sigma_t$ then $n = 1 + \frac{1}{m}$. Furthermore, if $\sigma_t \propto \ln s$ then $m = 1$ and $n = 2$, which corresponds just to the dipole Pomeron model. In the tripole Pomeron model $m = 2$ and $n = 3/2$, which means $\sigma_t \propto \ln^2 s$.

III. DIPOLE PARAMETRIZATIONS

The dominating term at high energy in this model is double pole

$$\varphi_d(j, t) \propto \frac{1}{(j-1-\alpha'_d t)^2}. \quad (11)$$

Apparently in accordance with the inequalities (10) the double pole obeys the unitarity limit for linear Pomeron trajectory ($m = 1$). Adding to the partial amplitude less singular term [simple pole with a trajectory having intercept $\alpha(0) = 1$ and a different slope α'] we obtain the dipole Pomeron model in the form

$$\varphi(j, t) = \eta(j) \frac{\beta_d(t)}{(j-1-\alpha'_d t)^2} + \eta(j) \frac{\beta_s(t)}{j-1-\alpha'_s t}. \quad (12)$$

It can be rewritten in (s, t) representation as

$$\begin{aligned} a(s, t) &= g_d \ln(-iz) (-iz)^{1+\alpha'_d t} \exp(b_d t) \\ &+ g_s (-iz)^{1+\alpha'_s t} \exp(b_s t), \end{aligned} \quad (13)$$

¹ t_{eff} can be defined by behavior of elastic scattering amplitude at $s \rightarrow \infty$. If $a(s, t) \approx s f(s) F(t/t_{\text{eff}}(s))$ then $\sigma_{el}(s) \propto |f(s)|^2 \int_{-\infty}^0 dt |F(t/t_{\text{eff}})|^2 = t_{\text{eff}} |f(s) F(1)|^2$.

where variable z is proportional to cosine of scattering angle in the t channel

$$z = (t + 2(s - 2m_p^2))/z_0, \quad z_0 = 1 \text{ GeV}^2. \quad (14)$$

Generally, the form factors (or residues) $\beta(t)$ may be chosen in various forms (e.g., exponential, factorized powers, etc.). However, we consider the simplest exponential ones.

Let us consider two effective reggeons: crossing-even, $R_+(s, t)$, and crossing-odd, $R_-(s, t)$ instead of four contributions— f , ω and ρ , a_2 (the latter two reggeons are of less importance at high energy). We take into account their contribution in the standard form. However, we insert an additional factor $Z_R(t)$ that changes sign at some t .²

$$R(s, t) = \eta_{RgR} Z_R(t) (-iz)^{\alpha_R(t)} \exp(b_R t), \quad (15)$$

where $\eta_{R+} = -1/\sin(0.5\pi\alpha_+(0))$ for R_+ reggeon and $\eta_{R-} = i/\cos(0.5\pi\alpha_-(0))$ for R_- reggeon. Obviously these terms are very close to f and ω reggeons, respectively. There are some arguments [13] to use the factors $Z_R(t)$ in the form

$$Z_R(t) = \frac{\tanh(1 + t/t_R)}{\tanh(1)}. \quad (16)$$

Going to extended wide regions of s ($\sqrt{s} \geq 5 \text{ GeV}$) and t ($0.1 \leq |t| \leq 6 \text{ GeV}^2$),³ we certainly need a few extra terms in amplitude to reach a good fit to the data. First of all it concerns the odderon contribution. The existing data on total cross section and parameters $\rho = \text{Re}a(s, 0)/\text{Im}a(s, 0)$, as is well known, do not show any visible odderon contribution. However, it appears definitely to provide the difference of pp and $\bar{p}p$ differential cross sections at $\sqrt{s} = 53 \text{ GeV}$ and t around the dip. So, we add the odderon contribution vanishing at $t = 0$

$$\begin{aligned} \mathcal{O}(s, t) = & t^2 z Z_{R-}(t) \{o_1 \ln^2(-iz) \exp(b_{o1} t) \\ & + o_2 \ln(-iz) \exp(b_{o2} t) \\ & + o_3 \exp(b_{o3} t)\} (-iz)^{1+\alpha'_o t}. \end{aligned} \quad (17)$$

The term $\propto \ln^2(s)$ in Eq. (17) does not violate unitarity restriction $\sigma_{el}(s) \leq \sigma_t(s)$ at very large s due to the presence of factor t^2 (in the dipole model $t_{\text{eff}} \sim 1/\ln s$, therefore $\sigma_{el} \propto t_{\text{eff}}^3 \ln^4 s \propto \ln s$).

At high energy and at $t = 0$ two main rescattering terms of dipole Pomeron (or cut terms) have the same form as the input amplitude—double pole plus simple pole. It means that comparing the model with experimental data we are

²For the crossing-odd term of amplitude such a factor is well known and describes the crossover effect, i.e., intersection of the ab and $\bar{a}\bar{b}$ differential cross sections at $t \approx -0.15 \text{ GeV}^2$. Our analysis [13] has shown that a similar factor is visible in the crossing-even reggeon term.

³A more sophisticated form for residues should be considered for larger $|t|$.

not able to distinguish unambiguously input terms and cuts. Then as a result, at $t = 0$ one may use the input amplitude only. At $t \neq 0$ the situation occurs more complicated because the slopes of trajectories in the cut terms are different from the input one. These terms are important at large $|t|$ but, in fact, they are already taken into account at $t = 0$.

Keeping in mind the above arguments and preserving a good description of the data at $t = 0$ we take Pomeron, Pomeron-Pomeron, and Pomeron-reggeons cuts vanishing at $t = 0$. Certainly they are not “genuine” rescatterings but mimic them quite efficiently at $t \neq 0$. Thus we write:

the Pomeron contribution

$$P(s, t) = -g_P (-iz)^{1+\alpha'_P t} [\exp(b_{P1} t) - \exp(b_{P2} t)], \quad (18)$$

the Pomeron-Pomeron cut

$$C_P(s, t) = -\frac{t}{\ln(-iz)} g_{PP} (-iz)^{1+\alpha'_P t/2} \exp(b_{PP} t), \quad (19)$$

the Pomeron-even reggeon cut

$$\begin{aligned} C_{R_+}(s, t) = & -\frac{t Z_{R_+}(t)}{\ln(-iz)} \eta_{R_+} g_{P+Z_{R_+}}(t) (-iz)^{\alpha_+(0)+\alpha'_{P+} t} \\ & \times \exp(b_{P+} t), \end{aligned} \quad (20)$$

where

$$\alpha'_{P+} = \frac{\alpha'_P \alpha'_{R_+}}{\alpha'_P + \alpha'_{R_+}}, \quad (21)$$

and the Pomeron-odd reggeon cut

$$\begin{aligned} C_{R_-}(s, t) = & -i \frac{t Z_{R_-}(t)}{\ln(-iz)} \eta_{R_-} g_{P-Z_{R_-}}(t) (-iz)^{\alpha_-(0)+\alpha'_{P-} t} \\ & \times \exp(b_{P-} t), \end{aligned} \quad (22)$$

$$\alpha'_{P-} = \frac{\alpha'_P \alpha'_{R_-}}{\alpha'_P + \alpha'_{R_-}}. \quad (23)$$

IV. TRIPOLE POMERON MODEL

As it follows from Eq. (10) for the dominating contribution in a tripole Pomeron model with $\sigma_t(s) \propto \ln^2(s)$, i.e., $n = 2$, $m = 3/2$, we should take

$$\varphi_1(j, t) = \eta(j) \frac{\beta_1(j, t)}{[(j-1)^2 - kt]^{3/2}}. \quad (24)$$

It seems to be natural to write the subleading terms as the following:

$$\varphi_2(j, t) = \eta(j) \frac{\beta_2(j, t)}{[(j-1)^2 - kt]}, \quad (25)$$

$$\varphi_3(j, t) = \eta(j) \frac{\beta_3(j, t)}{[(j-1)^2 - kt]^{1/2}}. \quad (26)$$

Then the amplitude has a form

$$\varphi(j, t) = \varphi_1(j, t) + \varphi_2(j, t) + \varphi_3(j, t) + R(j, t), \quad (27)$$

where $R(j, t)$ means the contribution of other reggeons and possible cuts (which are important at low energies).

Taking into account that

$$\int_0^\infty dx x^{\alpha-1} e^{-\omega x} J_\nu(\omega_0) = I_\nu^\alpha, \quad (28)$$

where

$$I_\nu^{\nu+1} = \frac{(2\omega_0)^\nu}{\sqrt{\pi}} \frac{\Gamma(\nu + 1/2)}{(\omega^2 + \omega_0^2)^{\nu+1/2}},$$

$$I_\nu^{\nu+2} = 2\omega \frac{(2\omega_0)^\nu}{\sqrt{\pi}} \frac{\Gamma(\nu + 3/2)}{(\omega^2 + \omega_0^2)^{\nu+3/2}},$$

one can find

$$\frac{1}{(\omega^2 + \omega_0^2)^{3/2}} = \frac{1}{2\omega_0} \int_0^\infty dx x e^{-x\omega} J_1(\omega_0 x), \quad (29)$$

$$\frac{1}{\omega^2 + \omega_0^2} = \frac{1}{\omega_0} \int_0^\infty dx x e^{-x\omega} \sin(x\omega_0), \quad (30)$$

and

$$\frac{1}{(\omega^2 + \omega_0^2)^{1/2}} = \int_0^\infty dx e^{-x\omega} J_0(\omega_0 x). \quad (31)$$

Thus tripole amplitude with the subleading terms can be presented as

$$a_{\text{tr}}(s, t) = iz \left\{ g_{+1} \exp(b_{+1}t) \ln(-iz) \frac{2J_1(\xi_+ \tau_+)}{\tau_+} \right. \\ \left. + g_{+2} \frac{\sin(\xi_+ \tau_+)}{\tau_+} \exp(b_{+2}t) \right. \\ \left. + g_{+3} J_0(\xi_+ \tau_+) \exp(b_{+3}t) \right\}, \quad (32)$$

where $\xi_+ = \ln(-iz) + \lambda_+$, z is defined by Eq. (14), and $\tau_+ = r_+ \sqrt{-t/t_0}$, $t_0 = 1 \text{ GeV}^2$, r_+ is a constant.

A similar expression for odderon contribution (but introducing the factors t and $Z_{R_-}(t)$) is given by

$$\mathcal{O}(s, t) = z t Z_{R_-}(t) \left\{ g_{-1} \ln(-iz) \frac{2J_1(\xi_- \tau_-)}{\tau_-} \exp(b_{-1}t) \right. \\ \left. + g_{-2} \frac{\sin(\xi_- \tau_-)}{\tau_-} \exp(b_{-2}t) \right. \\ \left. + g_{-3} J_0(\xi_- \tau_-) \exp(b_{-3}t) \right\}, \quad (33)$$

where $\xi_- = \ln(-iz) + \lambda_-$ and $\tau_- = r_- \sqrt{-t/t_0}$.

Again, similar to the dipole model we add the ‘‘soft’’ Pomeron

$$P(s, t) = -g_P (-iz)^{1+\alpha'_P t} \exp(b_P t), \quad (34)$$

the reggeon and cut contributions which are of the same form as in dipole Pomeron model Eqs. (19), (20), and (22).

AGLN model.—Let us give a few comments about another version of the tripole Pomeron model presented in the papers [6,7].

- (1) If $\xi = \ln(-is/s_0)$, $s_0 = 1 \text{ GeV}^2$, then the first Pomeron term in [6,7] is identical to the term in Eq. (32), while for the second and third terms the authors use

$$g_2(t) \xi J_0(\xi \tau)$$

and

$$g_3(t) [J_0(\xi \tau_+) - \xi_0 \tau_+ J_1(\xi \tau_+)],$$

which originated from the partial amplitudes

$$\varphi(j, t) = \eta(j) g_2(t) \frac{2(j-1)}{[(j-1)^2 - kt]^{3/2}},$$

and

$$\varphi(j, t) = \eta(j) g_2(t) \frac{(j-1)^2 + kt}{[(j-1)^2 - kt]^{3/2}},$$

respectively.

- (2) They used another form of odderon terms. The maximal odderon contribution in the form

$$\mathcal{O}_m(s, t) = g_{-1} \ln^2(-iz) \frac{\sin(\xi \tau_-)}{\tau_-} \exp(b_{-1}t) \\ + g_{-2} \ln(-iz) \cos(\xi \tau_-) \exp(b_{-2}t) \\ + g_{-3} \exp(b_{-3}t) \quad (35)$$

as well as a simple pole odderon and odderon-Pomeron cut are also taken into account.

- (3) Omitting the details we note that because of the chosen form of signature factors the AGLN amplitude has pole in the physical region at $t = -1/\alpha' = -4 \text{ GeV}^2$. This feature of the model restricts its applicability region. AGLN amplitude has similar poles even at lower values of $|t|$ in the reggeon terms. Thus the model requires a modification to describe a wider region of t than was considered in [7]; namely, $|t| \leq 2.6 \text{ GeV}^2$.

- (4) Clearly this model leads to the unreasonable intercept value for the crossing-odd reggeon, $\alpha_-(0) = 0.34$. It is in strong contradiction with the values known from meson resonance spectroscopy data. One could expect it close to the intercept of ω trajectory, $\alpha_\omega(0) \approx 0.43\text{--}0.46$ [11].

Nevertheless, in Sec. V we demonstrate the curves for differential cross sections obtained in the AGLN model in comparison with the results of our dipole and tripole models at energies available and future LHC.

V. COMPARISON WITH EXPERIMENTAL DATA

A. Total cross sections

Analyzing the pp and $\bar{p}p$ data we keep in mind a further extension of the models to elastic $\pi^\pm p$ and $K^\pm p$ scattering, which are quite precisely measured. One important point should be underlined from the beginning. Fitting the pp and $\bar{p}p$ data on σ_t and ρ gives the set of parameters which is essentially different from those derived from the fit of all (p , \bar{p} , π , and K meson) the data.

Following this procedure at the first stage we determine all the parameters that control the amplitudes at $t = 0$. We use the standard data set for the $\pi^\pm p$ and $K^\pm p$ total cross sections and the ratios ρ (at $5 \leq \sqrt{s} < 2000$ GeV) [15] to find intercepts of C_\pm reggeons and couplings of the reggeon and Pomeron exchanges. There are 542 experimental points in the region under consideration (see Table I).

TABLE I. Quality of the fit to σ_t and ρ .

Quantity	Number of data	χ^2_{tot}/N_p	
		Dipole model	Tripole model
σ_t^{pp}	104	$0.882\,60 \times 10^0$	$0.870\,55 \times 10^1$
$\sigma_t^{\bar{p}p}$	59	$0.952\,80 \times 10^0$	$0.962\,73 \times 10^0$
$\sigma_t^{\pi^+ p}$	50	$0.662\,16 \times 10^0$	$0.667\,92 \times 10^0$
$\sigma_t^{\pi^- p}$	95	$0.100\,23 \times 10^1$	$0.998\,64 \times 10^0$
$\sigma_t^{K^+ p}$	40	$0.723\,57 \times 10^0$	$0.721\,04 \times 10^0$
$\sigma_t^{K^- p}$	63	$0.613\,92 \times 10^0$	$0.608\,83 \times 10^0$
ρ^{pp}	64	$0.166\,12 \times 10^1$	$0.169\,65 \times 10^1$
$\rho^{\bar{p}p}$	11	0.40392×10^0	$0.406\,75 \times 10^0$
$\rho^{\pi^+ p}$	8	$0.151\,07 \times 10^1$	$0.150\,36 \times 10^1$
$\rho^{\pi^- p}$	30	$0.125\,60 \times 10^1$	$0.121\,22 \times 10^1$
$\rho^{K^+ p}$	10	$0.108\,69 \times 10^1$	$0.100\,16 \times 10^1$
$\rho^{K^- p}$	8	$0.121\,85 \times 10^1$	$0.116\,11 \times 10^1$
Total	542	$0.994\,50 \times 10^0$	$0.993\,45 \times 10^0$

TABLE II. Intercepts and couplings (GeV^{-2}) in the dipole and tripole models from the fit to σ_t and ρ .

Dipole model			Tripole model		
Parameter	Value	Error	Parameter	Value	Error
$\alpha_{R^+}(0)$	$0.808\,46 \times 10^0$	$0.360\,35 \times 10^{-2}$	$\alpha_{R^+}(0)$	$0.719\,47 \times 10^0$	$0.184\,96 \times 10^{-2}$
$\alpha_{R^-}(0)$	$0.465\,05 \times 10^0$	$0.914\,16 \times 10^{-2}$	$\alpha_{R^-}(0)$	$0.463\,56 \times 10^0$	$0.737\,46 \times 10^{-2}$
g_d^p	$0.894\,35 \times 10^1$	$0.194\,99 \times 10^0$	g_{+1}^p	$0.153\,30 \times 10^2$	$0.316\,19 \times 10^0$
g_s^p	$-0.521\,59 \times 10^2$	$0.300\,78 \times 10^1$	g_{+2}^p	$0.191\,53 \times 10^1$	$0.385\,89 \times 10^{-1}$
$g_{R^+}^p$	$0.158\,57 \times 10^3$	$0.308\,46 \times 10^1$	g_{+3}^p	$0.206\,72 \times 10^0$	$0.267\,47 \times 10^{-2}$
$g_{R^-}^p$	$0.589\,61 \times 10^2$	$0.287\,75 \times 10^1$	$g_{R^+}^p$	$0.969\,06 \times 10^2$	$0.846\,78 \times 10^0$
g_d^π	$0.704\,77 \times 10^1$	$0.227\,19 \times 10^0$	$g_{R^-}^p$	$0.592\,94 \times 10^2$	$0.232\,28 \times 10^1$
g_s^π	$-0.457\,20 \times 10^2$	$0.290\,22 \times 10^1$	g_{+1}^π	$0.699\,01 \times 10^1$	$0.183\,96 \times 10^0$
$g_{R^+}^\pi$	$0.106\,91 \times 10^3$	$0.335\,90 \times 10^1$	g_{+2}^π	$0.101\,06 \times 10^1$	$0.271\,23 \times 10^{-1}$
$g_{R^-}^\pi$	$0.107\,10 \times 10^2$	$0.525\,07 \times 10^0$	$g_{R^+}^\pi$	$0.562\,96 \times 10^2$	$0.453\,60 \times 10^0$
g_d^K	$0.543\,51 \times 10^1$	$0.292\,05 \times 10^0$	$g_{R^-}^\pi$	$0.107\,84 \times 10^2$	$0.436\,87 \times 10^0$
g_s^K	$-0.297\,03 \times 10^2$	$0.332\,34 \times 10^1$	g_{+1}^K	$0.121\,86 \times 10^2$	$0.224\,24 \times 10^0$
$g_{R^+}^K$	$0.707\,85 \times 10^2$	$0.437\,92 \times 10^1$	g_{+2}^K	$0.146\,83 \times 10^0$	$0.304\,39 \times 10^{-1}$
$g_{R^-}^K$	$0.236\,74 \times 10^2$	$0.111\,59 \times 10^1$	$g_{R^+}^K$	$0.287\,30 \times 10^2$	$0.510\,47 \times 10^0$
			$g_{R^-}^K$	$0.238\,31 \times 10^2$	$0.916\,97 \times 10^0$

An extension of the $pp \rightarrow pp$ and $\bar{p}p \rightarrow \bar{p}p$ dipole and tripole amplitudes to $\pi^\pm p$ and $K^\pm p$ elastic scattering is quite straightforward. All the couplings vary in these amplitudes at $t = 0$, but the odderon does not contribute to the πp and $K p$ amplitudes. In the simplest unitarization schemes (eikonal, U matrix) all total cross sections at asymptotically high energies have the universal behavior $\sigma_t(s) \rightarrow \sigma_0 \log^2(s_{ap}/s_0)$, where σ_0 is independent of the initial particles. Today the data available support this conclusion and advocate putting the same couplings $g_{+1}^p = g_{+1}^\pi = g_{+1}^K$ for the leading Pomeron terms in all amplitudes. Additionally, in order to avoid uncertainty at $t = 0$ [constant contributions to total cross sections come additively from the third term of Eq. (32) and from soft Pomeron, Eq. (34)], we substitute couplings g_{+3} for $g_{+3} - g_p$ in Eq. (32). As a result we have energy independent contribution to the total cross from g_{+3} only.

The following normalization of $ab \rightarrow ab$ amplitude is used,

$$\sigma_t = \frac{1}{s_{ab}} \text{Im}A(s, 0), \quad \frac{d\sigma}{dt} = \frac{1}{16\pi s_{ab}^2} |A(s, t)|^2, \quad (36)$$

where

$$s_{ab} = \sqrt{(s - m_a^2 - m_b^2)^2 - 4m_a^2 m_b^2} = 2p_a^{\text{lab}} \sqrt{s}$$

and p_a^{lab} is the momentum of hadron a in laboratory system of b .

The details of the fit at $t = 0$ are presented in Tables I and II.

B. Differential cross sections

At the second stage of the fitting procedure we fix all the intercept and coupling values obtained at the first stage. The other parameters are determined by fitting the $d\sigma/dt$ data in the region

TABLE III. Quality of the fit to $d\sigma/dt$.

	Number of points, N_p	χ^2_{tot}/N_p	
		Dipole model	Tripole model
$d\sigma^{pp}/dt$	1857	0.15122×10^1	0.18153×10^1
$d\sigma^{\bar{p}p}/dt$	675	0.14183×10^1	0.16697×10^1

$$0.1 \leq |t| \leq 6 \text{ GeV}^2, \quad \sqrt{s} \geq 5 \text{ GeV}. \quad (37)$$

The measurements of the differential elastic cross sections were very intensive for the past 40 years. Fortunately, most of them have been collected in the Durham database [16]. However, there are 80 papers with different conventions and various units. The complete list of the references is given by [13]. We have uniformly formatted them, found and corrected some errors in the sets, and gave a detailed description of a full set which contains about 10 000 points. Analyzing each subset of these data, we have paid [13] particular attention to the data at small t . Some of the subsets that are in strong disagreement with the rest of the data set were excluded from the fit.

TABLE IV. Parameters of the models, from the fit to $d\sigma/dt$ (parameters r_{\pm} , λ_{\pm} are dimensionless, $t_{R\pm}$ are given in GeV^2 , the rest of the parameters are given in GeV^{-2}).

Dipole model			Tripole model		
Parameter	Value	Error	Parameter	Value	Error
α'_d	0.30631×10^0	0.16923×10^{-2}	r_+	0.25417×10^0	0.33181×10^{-2}
α'_s	0.28069×10^0	0.19026×10^{-3}	λ_+	0.11575×10^1	0.14824×10^0
b_d	0.38675×10^1	0.22767×10^{-1}	b_{+1}	0.34583×10^1	0.37982×10^{-1}
b_s	0.55679×10^0	0.14694×10^{-2}	b_{+2}	0.19091×10^1	0.30598×10^{-1}
α'_{R+}	0.82000×10^0	Fixed	b_{+3}	0.45970×10^0	0.29750×10^{-2}
b_{R+}	0.29226×10^1	0.30019×10^{-1}	α'_{R+}	0.82000×10^0	Fixed
t_{R+}	0.48852×10^0	0.26683×10^{-2}	b_{R+}	0.10668×10^1	0.30350×10^{-1}
α'_{R-}	0.91000×10^0	Fixed	t_{R+}	0.54237×10^0	0.13817×10^{-1}
b_{R-}	0.15201×10^1	0.68671×10^{-1}	α'_{R-}	0.91000×10^0	Fixed
t_{R-}	0.14497×10^0	0.24811×10^{-2}	b_{R-}	0.61435×10^{-1}	0.20044×10^{-1}
o_1	0.30738×10^0	0.31368×10^{-2}	t_{R-}	0.15755×10^0	0.26068×10^{-2}
o_2	-0.63119×10^1	0.55282×10^{-1}	r_-	0.78807×10^{-1}	0.60563×10^{-2}
o_3	0.13456×10^0	0.21551×10^{-2}	λ_-	0.16281×10^2	0.19020×10^1
α'_o	0.21810×10^{-1}	0.70324×10^{-3}	o_1	-0.56075×10^{-1}	0.51702×10^{-2}
b_{o1}	0.39317×10^1	0.81697×10^{-2}	o_2	0.17372×10^1	0.17893×10^0
b_{o2}	0.45007×10^1	0.76861×10^{-2}	o_3	-0.61193×10^2	0.36330×10^1
b_{o3}	0.12947×10^1	0.76773×10^{-2}	b_{o1}	0.12038×10^1	0.26425×10^{-1}
g_P	0.58961×10^2	0.98576×10^{-1}	b_{o2}	0.15152×10^1	0.31722×10^{-1}
α'_P	0.30696×10^0	0.20475×10^{-3}	b_{o3}	0.26331×10^1	0.78349×10^{-1}
b_{P1}	0.54894×10^0	0.15036×10^{-2}	g_P	0.16042×10^2	0.13856×10^{-1}
b_{P2}	0.59365×10^1	0.34863×10^{-1}	α'_P	0.36060×10^0	0.76335×10^{-2}
g_{PP}	-0.39324×10^2	0.36883×10^0	b_P	0.14662×10^1	0.29152×10^{-1}
b_{PP}	0.11828×10^1	0.44025×10^{-2}	g_{PP}	0.91195×10^1	0.84044×10^0
g_{P+}	-0.22656×10^3	0.27529×10^1	b_{PP}	0.44977×10^0	0.46404×10^{-1}
b_{P+}	0.17522×10^1	0.98459×10^{-2}	g_{P+}	0.11772×10^2	0.57753×10^{-1}
g_{P-}	-0.15255×10^2	0.28213×10^0	b_{P+}	0.81585×10^{-1}	0.28185×10^{-1}
b_{P-}	0.24068×10^{-1}	0.61336×10^{-2}	g_{P-}	0.81908×10^1	0.88408×10^0
			b_{P-}	-0.79115×10^{-1}	0.45833×10^{-1}

A similar work has been done for the data at $|t| > 0.7 \text{ GeV}^2$. We have found out and corrected some mistakes in the database. Furthermore, we excluded from the final data set the subsets [17] at $\sqrt{s} = 9.235 \text{ GeV}$, [18] at $\sqrt{s} = 19.47$ and 27.43 GeV , [19] at $\sqrt{s} = 53.0$ from pp data, and [20] at $\sqrt{s} = 7.875 \text{ GeV}$, [21] at $\sqrt{s} = 9.778 \text{ GeV}$ from $\bar{p}p$ data because they strongly contradict the bulk of data. Thus, the considered models were fitted to 2532 points of $d\sigma/dt$ in the region Eq. (37). The results are given in Table III for a quality of fitting and in Table IV for the fitting parameters.

In Figs. 1–5 we show experimental data at some energies and theoretical curves obtained in three models: AGLN [7], dipole, and tripole. As for the AGLN model, we would like to emphasize that the corresponding curves were calculated at the parameters given in [7]. However, in contrast to dipole and tripole models, the AGLN model was fitted to differential cross sections at $\sqrt{s} > 9.7 \text{ GeV}$ and $|t| < 2.6 \text{ GeV}^2$ but not with a complete data set. Therefore a disagreement between curves and data behaviors at lowest energies is not surprising in the given model. The AGLN model works well at high energies.

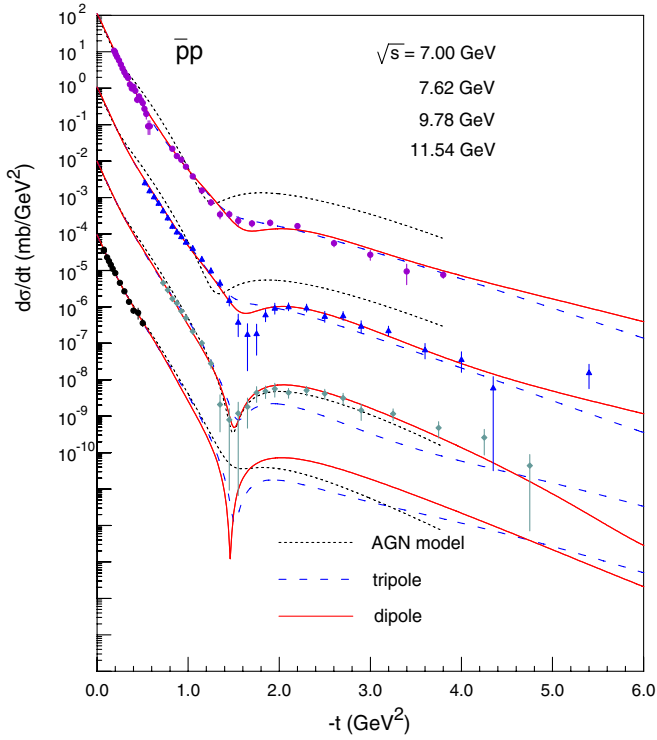


FIG. 1 (color online). $\bar{p}p$ at low energies.

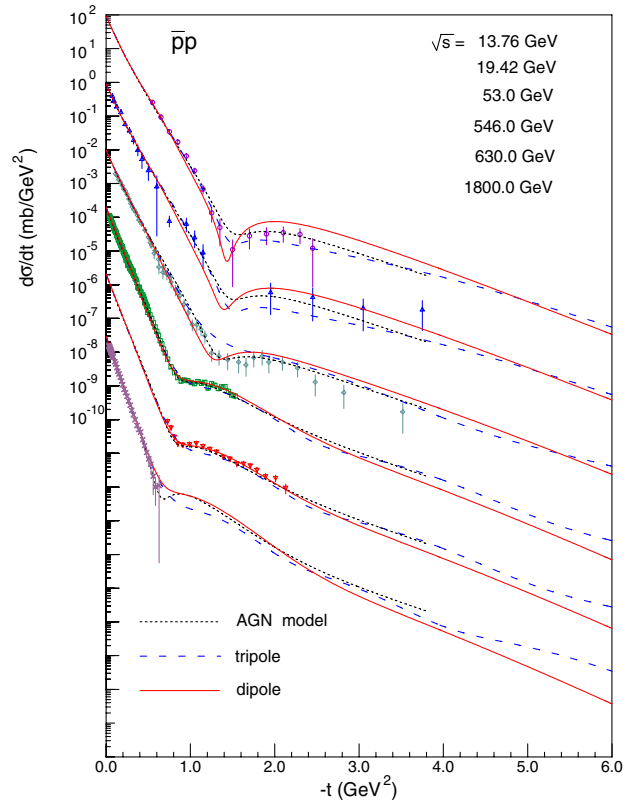


FIG. 3 (color online). $\bar{p}p$ at high energies.

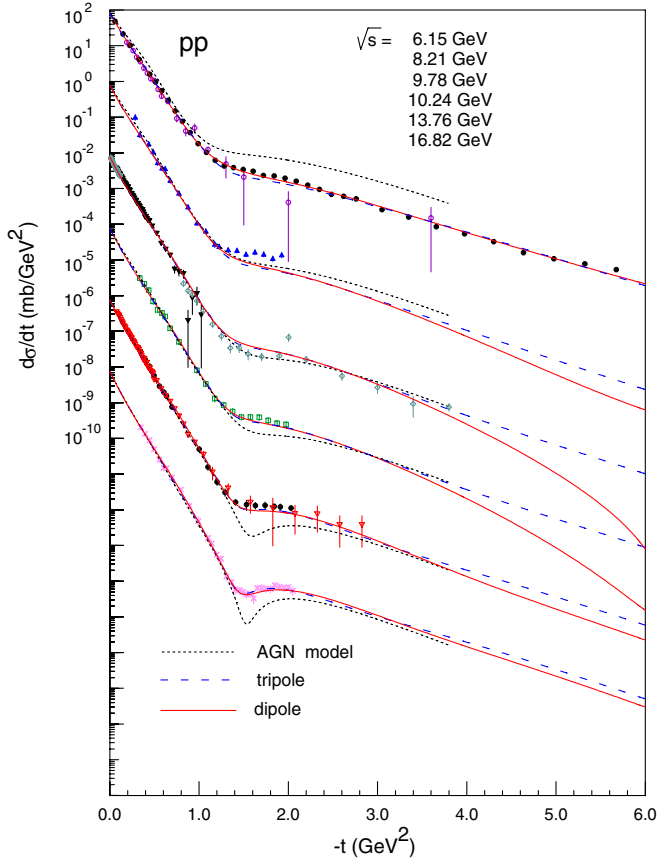


FIG. 2 (color online). pp at low energies.

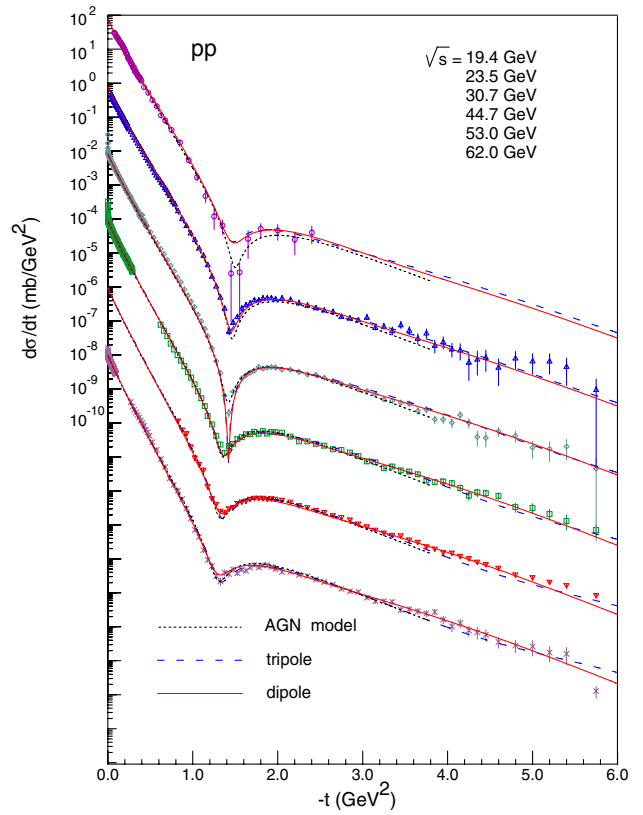


FIG. 4 (color online). pp at high energies.

VI. CONCLUSION

In this paper we compare three unitarized models of elastic scattering amplitude fitting the dipole and tripole models to all existing data. We emphasize that the amplitude leading to the behavior of $\sigma_t \propto \ln^2 s$ should be parametrized with special care of the unitarity and analyticity restrictions on properties of the leading partial wave singularity.

The figures and tables demonstrate a good description of the data within the considered models. However, the obtained χ^2 (Table III) hints that the dipole Pomeron model looks more preferable.

We believe the most interesting and instructive result for a further search of a more realistic model is shown in Fig. 5. Our predictions of the compared models (together with the AGLN model) for pp cross section at LHC energy are crucially different at $|t|$ around 0.3–0.5 GeV^2 . Certainly the future TOTEM measurement will allow one to distinguish between three considered models.

ACKNOWLEDGMENTS

I would like to thank Professor B. Nicolescu and Dr. J. R. Cudell for many useful discussions. The work was supported partially by the Ukrainian Fund of Fundamental Researches.

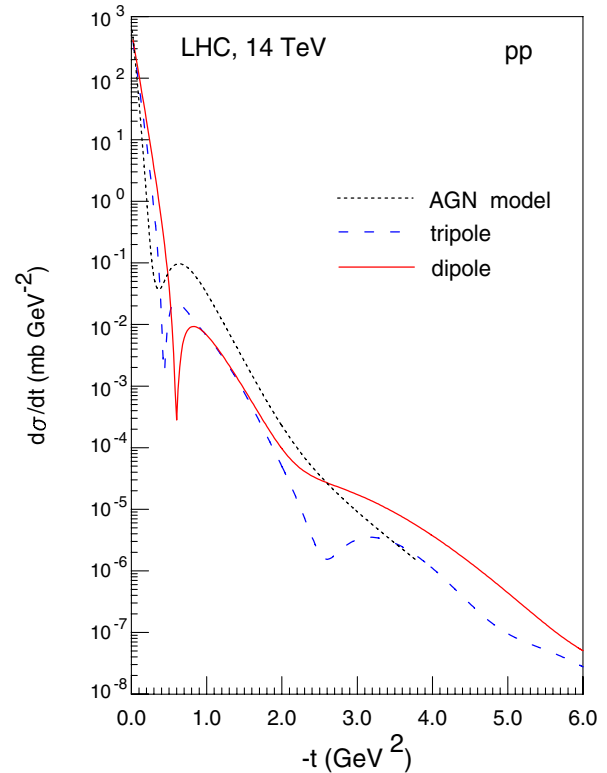


FIG. 5 (color online). Predictions for LHC energy.

- [1] A. Donnachie and P. V. Landshoff, *Phys. Lett. B* **296**, 227 (1992); P. V. Landshoff, arXiv:hep-ph/0509240; *Nucl. Phys. B, Proc. Suppl.* **99A**, 311 (2001), and references therein.
- [2] M. Giffon, P. Desgrolard, and E. Predazzi, *Z. Phys. C* **63**, 241 (1994).
- [3] Discussion of an eikonal approximation in the Regge theory as well as references to the original papers on this subject can be found in P.D.B. Collins, *An Introduction to Regge Theory & High Energy Physics* (Cambridge University Press, Cambridge, 1977); see also K. A. Ter-Martirosyan, *JETP Lett.* **15**, 734 (1972); V. A. Petrov and A. V. Prokudin, *Eur. Phys. J. C* **23**, 135 (2002); C. Bourrely, J. Soffer, and T. T. Wu, *Eur. Phys. J. C* **28**, 97 (2003); P. A. S. Carvalho, A. F. Martini, and M. J. Menon, *Eur. Phys. J. C* **39**, 359 (2005).
- [4] S. M. Troshin and N. E. Tyurin, *Phys. Part. Nucl.* **35**, 555 (2004); arXiv:hep-ph/0308027, and references therein; L. L. Jenkovszky, B. V. Struminsky, and A. N. Wall, *Sov. J. Part. Nucl.* **19**, 180 (1988).
- [5] L. Lukaszuk and B. Nicolescu, *Lett. Nuovo Cimento Soc. Ital. Fis.* **8**, 405 (1973); P. Gauron, E. Leader, and B. Nicolescu, *Nucl. Phys.* **B299**, 640 (1988).
- [6] P. Gauron, E. Leader, and B. Nicolescu, *Phys. Lett. B* **238**, 406 (1990).
- [7] R. Avila, P. Gauron, and B. Nicolescu, *Eur. Phys. J. C* **49**, 581 (2007).
- [8] L. L. Jenkovszky, E. S. Martynov, and B. V. Struminsky, *Phys. Lett. B* **249**, 535 (1990).
- [9] P. Desgrolard, M. Giffon, E. Martynov, and E. Predazzi, *Eur. Phys. J. C* **18**, 359 (2000).
- [10] J. R. Cudell *et al.*, *Phys. Rev. D* **65**, 074024 (2002); *Phys. Rev. Lett.* **89**, 201801 (2002); arXiv:hep-ph/0206172.
- [11] P. Desgrolard, M. Giffon, E. Martynov, and E. Predazzi, *Eur. Phys. J. C* **18**, 555 (2001).
- [12] J. R. Cudell, E. Martynov, and O. Selyugin, *Eur. Phys. J. C* **33**, s533 (2004); arXiv:hep-ph/0311019.
- [13] J. R. Cudell, E. Martynov, O. Selyugin, and A. Lengyel, *Phys. Lett. B* **587**, 78 (2004).
- [14] J. R. Cudell, A. Lengyel, and E. Martynov, *Phys. Rev. D* **73**, 034008 (2006).
- [15] S. Eidelman *et al.*, *Phys. Lett. B* **592**, 1 (2004); Encoded data files are available at <http://pdg.lbl.gov/2005/hadronic-xsections/hadron.html>.
- [16] M. R. Whalley *et al.* [Durham Database Group (UK)], <http://durpdg.dur.ac.uk/hepdata/reac.html>.
- [17] C. Bruneton *et al.*, *Nucl. Phys.* **B124**, 391 (1977).
- [18] S. Conetti *et al.*, *Phys. Rev. Lett.* **41**, 924 (1978).
- [19] J. C. M. Armitage *et al.*, *Nucl. Phys.* **B132**, 365 (1978).
- [20] M. Y. Bogolyubsky *et al.*, *Sov. J. Nucl. Phys.* **41**, 773 (1985).
- [21] C. W. Akerlof *et al.*, *Phys. Rev. D* **14**, 2864 (1976).